Early cementation and accommodation space dictate the evolution of an overstepping barrier system during the Holocene

Giovanni De Falco [a,*], Fabrizio Antonioli [b], Giorgio Fontolan [c], Valeria Lo Presti [d], Simone Simeone [a], Renato Tonielli [e]

[a] Istituto per l'Ambiente Marino Costiero CNR, Località Sa Mardini, 09170 Torregrande Oristano, Italy
[b] Enea — Unit for Environment and Energy Modeling, via Anguillarese 301, 00123 Roma, Italy
[c] Dipartimento di Matematica & Geoscienze, Università degli Studi di Trieste, via E. Weiss, 2-34128 Trieste, Italy
[d] Università degli Studi La Sapienza Roma, Piazzale Aldo Moro 5, 00185 Roma, Italy
[e] Istituto per l'Ambiente Marino Costiero CNR, Calata Porta di Massa Interno Porto, 80133 Napoli, Italy

ARTICLE INFO

Accepted 1 August 2015

Keywords:
Barrier
Beachrocks
Lagoon
Antecedent topography
Relative sea-level rise
Flooding

ABSTRACT

The morphology and stratigraphic features of a well-preserved drowned barrier system, located on the western coast of Sardinia (Mediterranean Sea), are presented here. The barriers were mapped using a multibeam echosounder. The Digital Terrain Model of the seabed revealed five sub-parallel barriers in a depth range of 18–37 m, with a distance of ~300 m between each single barrier. Direct inspection by scuba diving, revealed that the barriers consist of beachrocks, topped by seagrass meadows growing on a biogenic hardground. The inner-most barrier is limited landward by a steep cliff, 10 m high, bordering the back-barrier area. About 200 km of seismic lines were collected along the barrier system using a 0.4–1.0 kJ sparker source and a 3.5 kHz Chirp Subbottom profiler. The seismic data, calibrated with vibrocores, allowed us to recognize the subaerial topographic surface of the last glacial maximum as well as several seismic units interpreted as the Pliocene marine sediments, the pre-Holocene deposits and the Holocene barrier–lagoon complex composed of shoreface, barrier, lagoonal/deltaic and beach deposits.

Despite the relatively high seabed gradient (0.3°–0.4°) and the relatively low rate of sea-level rise (10–15 mm y^{-1}), the barriers were well preserved due to the early diagenetic processes which led to a rapid cementation with the formation of beachrocks, and the subsequent overstepping with the rise of the sea level. The development of the overstepping barrier system is strictly related to the antecedent subaerial topography which is, in turn, related to the tectonic setting of the area. The Pliocene seismic unit was lowered by a direct fault at the entrance of the gulf forming a depression filled by sediments. The overstepping barrier system developed following the increase of the seabed gradient and was limited landward by the above-mentioned depression which increased the accommodation space. Following the sea-level rise and the barrier formation, this depression was filled by lagoonal sediments, washover fans and sediments coming from the rivers.

The age model of barrier evolution, based on previous sea-level-rise curves during the Holocene, supported by radiocarbon data, highlighted that the whole system evolved over a time period of 1 ka; while the time elapsed from this formation to the drowning of single barriers was estimated to be in the order of magnitude of centuries. Scenarios of short-term evolution of modern barrier–lagoon systems of the adjacent coastal sector, under conditions of accelerated sea-level rise, according to Church et al. (2013) (2013 IPCC report) and Rahmstorf (2007) projections, were elaborated. The study of this ancient analogue suggests that the processes of adaptation of coastal systems to the rising sea level would require times evaluable from centuries to millennia.

1. Introduction

Late Quaternary barrier–lagoon systems that migrate landward as sea level rises have been found in several sites over clastic transgressive coasts (e.g., Swift, 1968; Belknap and Kraft, 1981; Nummedal and Swift, 1987). Understanding their dynamics is essential since they provide well-documented ancient analogues to possible future scenarios of coastal evolution under conditions of accelerated sea-level rise.

The term 'coastal barrier' for modern coastlines, has been used to refer to different geomorphological features from its early definitions to the recent scientific literature. Otvos (2012) reviewed the nomenclature and classification issues of coastal barriers considering two basic types: 1) barrier islands, a physiographic, hydrographic, sedimentary

* Corresponding author.
E-mail addresses: giovanni.defalco@cnr.it (G. De Falco), fabrizio.antonioli@enea.it (F. Antonioli), fontolan@units.it (G. Fontolan), valeria.lopresti@uniroma1.it (V. Lo Presti), simone.simeone@iamc.cnr.it (S. Simeone), renato.tonielli@cnr.it (R. Tonielli).

and ecological boundary parallel to the shore which is located between the inshore and open marine environments, and 2) barrier spits, which are linked to the mainland shore at their updrift terminus, and may partially close the entrance of narrow, elongated lagoons parallel to the shore (Otvos, 2012). Modern barrier islands are extended worldwide along 20,783 km of coastline, 10% of all continental shorelines, mainly along wave-dominated coasts, which were subjected to a rising sea level in the late Holocene (5 ka BP to present) (Stutz and Pilkey, 2011).

Barrier–lagoon systems include the shoreface sector, the barrier and the back-barrier sector, where washover fans and lagoons develop (Mellett et al., 2012; Otvos, 2012).Their formation is related to the interplay between wave energy, sediment supply, accommodation space and rate of relative sea-level rise (Hesp and Short, 1999).

In particular, barriers and back-barrier–lagoons can develop when the substrate gradient ranges between 0.05° and 0.8° (Roy et al., 1994). The barrier development, type and stability depend on the amount of sediment available to build them and on the quality of sediment supplied to the system. Barrier islands receiving a surplus of sandy sediment may grow to considerable length and width, whereas barriers receiving mud-rich sediments tend to be narrow (Stutz and Pilkey, 2011).

Wave energy is essential for barrier formation. Most extensive barriers are formed along wave-exposed coasts, but they also exist in fetch-limited environments (Pilkey et al., 2009). The relative importance of storm waves on barrier islands may be predicted by the ration of the maximum storm wave height relative to the mean height (Stutz and Pilkey, 2011). Higher ratios (>5), typical of Arctic islands, are associated with storm-dominated barriers, while lower ratios (<3), typical of tropical islands, are associated with barriers evolved in response to fair-weather swells (Stutz and Pilkey, 2011). Intermediate ratios (3–5) are generally typical of temperate barrier systems. Overwash and inlet formation are frequent in storm-dominated settings, particularly along microtidal coasts (Hayes, 1979).

Sea-level rise is one of the main processes which led to the formation of present-day barriers (Swift, 1975) and rapid increases in the sea level may lead to barrier breakup and drowning (Carter et al., 1989; Storms and Swift, 2003; Lorenzo-Trueba and Ashton, 2014).

Another relevant factor which controls the barrier development is geological inheritance. This controls the accommodation space for sediments in terms of coastal geomorphological setting and topography of the transgressive surface (Belknap and Kraft, 1981; Evans et al., 1985). Barrier behavior is sensitive to changes in the back-barrier slope (Storms and Swift, 2003), and barrier drowning is more likely in flatter back-barrier surfaces (Lorenzo-Trueba and Ashton, 2014).

The preservation potential of drowned barriers and related transgressive deposits is considered relatively low in comparison to the deposits associated with regressive coasts (Storms and Swift, 2003). Two basic models of barrier retreat under transgressive conditions were proposed: (i) the rollover model is generally considered the dominant retreat process, and involves a continuous migration of the barrier systems following the shoreline retreat, with the reworking of shoreface and barrier deposits and the absence of deposit preservation offshore (Swift and Moslow, 1982; Leatherman et al., 1983); (ii) the barrier retreat through overstepping involves a partial preservation of transgressive deposits or barrier morphology following a fast rate of sea-level rise (Rampino and Sanders, 1980, 1982, 1983; Forbes et al., 1991; Storms et al., 2008; Mellett et al., 2012). In particular, gravel barriers are more likely to be preserved (Long et al., 2006; Mellett et al., 2012).

The acquisition of high resolution multibeam echosounder data during the last decades highlighted the occurrence of preserved morphology of overstepped barriers along some shelf sites, such as the Gulf of Mexico-North West Florida (Gardner et al., 2005, 2007), the Adriatic Sea (Storms et al., 2008), and the KwaZulu-Natal — Durban continental shelf, South Africa (Green et al., 2013; Salzmann et al., 2013). Meanwhile, the occurrence of barrier–lagoon transgressive deposits was revealed by seismic surveys and vibro-coring (Rampino and Sanders, 1980; Storms et al., 2008; Mellett et al., 2012), but there generally is a scarcity of examples of well-preserved drowned systems.

The cementation of beach deposits, forming the so-called beachrocks (Vousdoukas et al., 2007), may favor the preservation of barrier morphology and related transgressive deposits (Green et al., 2013; Salzmann et al., 2013). Beachrocks are currently found in tropical/subtropical and low temperate latitudes, and microtidal coasts (Vousdoukas et al., 2007). In the Mediterranean sea, their presence is only reported in the eastern basin. However, several examples of Late Pleistocene–Holocene beachrocks, used as markers of the last sea level rise, were also reported in the western basin (Demuro and Orrù, 1998; Mauz et al., 2015).

In this paper, we show a case study of a well-preserved transgressive barrier–lagoon system located in a high wave energy area (Cucco et al., 2006), the western Mediterranean, formed by overstepping barriers and back-barrier deposits. The coupling of geophysical data (multibeam and seismic), sediment (vibrocores, grab samples) and radiocarbon data, provided a detailed paleo-environmental reconstruction of the evolution of such a barrier–lagoon system.

The specific aims of the paper are (i) to show how barrier cementation and the topography of the pre-existing surface influenced the formation and retreat through overstepping of a transgressive barrier–lagoon system during early Holocene; (ii) to infer the time interval and the sea-level variation which occurred from the formation of the system up to their definitive drowning; and (iii) to infer possible future evolution scenarios of the adjacent coast under conditions of accelerated sea-level rise, based on this well-documented ancient analogue.

2. Regional setting

The study area is located along the inner shelf of western Sardinia (western Mediterranean Sea), at the entrance of the Gulf of Oristano (Fig. 1). The gulf has a surface area of approximately 150 km^2, and is bordered to the West by two rocky capes. The sandy shores are composed of barrier–lagoon systems, sandy spits, and attached barriers while the backshore is an alluvial plane with lagoons and dune systems. Several inlets allow for the connection between the lagoons and the sea. The Tirso river, whose mouth is located in the northeastern sector of the gulf, is the main source of sediments from the land. The inland plane was deeply modified during the past century by heavy drainage works and water channelization in order to promote the use of the land for agriculture.

The gulf represents the western boundary of the Campidano graben, a Pliocene–Quaternary structural depression which is oriented NW–SE. This basin is a half-graben with the main depocenter located in the Gulf of Oristano. It is bordered by an eastward dipping master fault located between the two capes of the gulf (Casula et al., 2001). The geological setting of the emerged land includes a Neogene sequence of marine sedimentary and volcanic formation outcropping in the Sinis Peninsula to the north and Cape Frasca to the south, overlying the Hercynian basement. Eastward, in the Campidano area, continental, brackish and marine Quaternary deposits occur.

The upper terms of the Neogene marine sequence, composed of Early Pliocene marine deposits, were found offshore the gulf entrance, below a thin layer of Quaternary sediments (Francolini et al., 1990; Lecca, 2000). Eastward, the Neogene marine sequence is tectonically dropped down and a thick succession of Pliocene–Quaternary deposits fills the gulf basin (Casula et al., 2001).

The gulf seafloor is colonized by two meadows of the seagrass *Posidonia oceanica* down to a depth of 15 m, separated by a barren channel running from the entrance of the gulf to the Tirso river mouth where deltaic river deposits are found (De Falco et al., 2006, 2008). The northern meadow is planted over a biogenic sedimentary substrate composed of carbonate sediments. The wider meadow is located in the central sector and is planted over coarse siliciclastic sediments derived from the wave winnowing of alluvial deposits (De Falco et al., 2008).

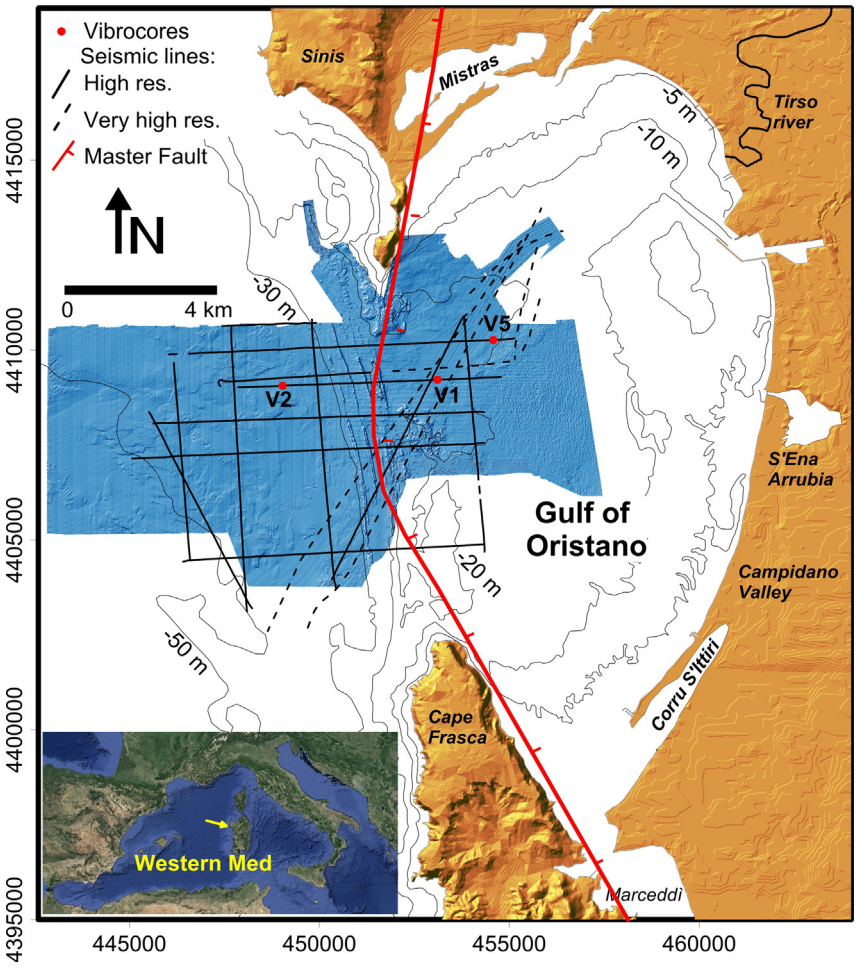

Fig. 1. Map of the study area showing the Digital Terrain Model of the seabed derived by the multibeam survey, the seismic lines and the location of the vibrocore sampling points. The position of the master fault at the entrance of the Gulf of Oristano is from Casula et al. (2001).

A morphological threshold characterizes the gulf entrance (De Falco et al., 2010). Outside the gulf, the superficial sediment distribution is composed of a pattern of siliciclastic sand and gravel sediments alternated with medium sands which have a mixed siliciclastic–carbonate composition (De Falco et al., 2010).

Many data have been recently published concerning the relative sea-level change in the western Mediterranean and particularly in Sardinia, during the last interglacial MIS 5.5. In Sardinia, where the last interglacial maximum altitude has the lowest variability among the Italian coastline (between 2–11 m), more than 60 MIS 5.5 sites are known. Therefore, Sardinia was chosen as a reference site for the MIS 5.5 eustatic elevation (Lambeck et al., 2004; Ferranti et al., 2006). Within this generally stable setting, minor but consistent patterns of vertical motions were detected on a scale of meters. Extremely slow subsidence occurs on the NW coast (Capo Caccia, Ferranti et al., 2006), indicative of block motion possibly accommodated by fault creeping or sliding associated with the Ligurian continental margin. On the other hand, in the Gulf of Orosei (Eastern Sardinia), the MIS 5.5 tidal notch shows a minor but continuous uplift between 7 and 11.5 m due to volcanic activity (Ferranti et al., 2006; Mariani et al., 2009). Archeological markers from many coastal sites in Sardinia, which were dated between 7.3 and 1.65 ka cal BP, have been used to infer the sea-level change during the late Holocene (Antonioli et al., 1997, 2007; Lambeck et al., 2011; Orrù et al., 2011, 2014; Di Rita and Melis, 2013). The vertical positioning of these archaeological markers with respect to their inferred ages indicates Late Holocene stability or weak uplift at 0.15 mm y^{-1}. A 30 m sediment core, collected in Southern Sardinia, showed Holocene subsidence at an average rate of 0.2 mm y^{-1}, due to sediment compaction (Antonioli et al., 2007).

Late Pleistocene deposits are present along the coastline to the northwest of the Gulf of Oristano, and a fossiliferous deposit containing fauna dated MIS 5.5 with the amino-stratigraphic method (Carboni and Lecca, 1985; Ulzega and Hearty, 1986; Davaud et al., 1991; Kindler et al., 1997) outcrops up to an elevation of 6 m. In the same area, Antonioli et al. (2007) analyzed several archeological markers (quarries and tombs) up to −1.85 m from the Punic and Roman age. The comparison with the curve of sea-level rise predicted by Lambeck et al. (2004) allows us to consider the study area which was stable since 2.35 ka BP.

Western Sardinia is considered one of the highest wave-energy coasts of the whole Mediterranean Sea. The dominant wind of the area is the Mistral, which arrives from the northwest (sectors between 300° and 315°, nautical convention) and comprises 70% of wind events with an intensity higher than 10 m s^{-1} (Cucco et al., 2006). A typical Mistral wind storm with a return period of 1 y produces a JONSWAP-type spectrum characterized by a significant wave height (WHS) of 8 m, a peak period of 10 s and a peak wave direction of 308° (northwest). Storms with a return period of 10 y are characterized by a WHS of 10 m and a peak period of 11.5 s. The strong wave hydrodynamics were related to the presence of active sorted bedforms at a depth of 43–70 m along the shelf offshore the gulf (De Falco et al., 2015). The yearly tides are very weak and the maximum water displacement in the absence of wind and regular pressure is <0.2 m (Simeone et al., 2014).

3. Methods

3.1. Multibeam echosounder data and direct seabed observations

Our research integrated the multibeam echosounder (MBES) data already published in De Falco et al. (2010) with new data acquired in 2013 during the ocean cruise SONOS 2013 on the R/V Urania of the Italian National Research Council (CNR). The new data were acquired using the Kongsberg EM 710, operating at a sonar frequency of 100 kHz, with a footprint of 0.5–1.2 m in a depth range of 15–50 m. The Digital Terrain Model (DTM) was elaborated at a spatial resolution of 2.5 m. This new MBES dataset integrates previous data acquired at the entrance of the Gulf of Oristano during 2007, using a Seabat-Reson 8111 device (see De Falco et al., 2010, for a detailed description of MBES data acquisition and processing). The Reson 8111 provided data with lower resolution allowing for the production of a DTM at 5 m of spatial resolution.

All data were processed using the software Caris Hips and Sips. The visualization of seabed morphology was obtained using the software Global Mapper and Golden Software Surfer 10.

Direct observations were obtained by dive inspections and using a subaqueous Remote Operating Vehicle (ROV) which allowed us to obtain videos and photographs of the seabed. The dive inspection was planned in the inner barrier along a route which started from the back barrier region and crossed the barrier crest. During the dive inspection beachrock samples and photographs of the seabed were collected and in situ observations of seafloor morphology and stratigraphy were annotated.

3.2. Seismic data

About 200 km of high-resolution seismic reflection profiles were collected in the study area, with a Geotech multi-tip spark array (MTSA) (Fig. 1). The Geotech MTSA source was sparking at 0.4–1 kJ, and data were processed with debias correction, filtering and gain corrections. The conversion of two-way travel time to real depth was obtained assuming an average velocity of 1550 ms^{-1} within the first 300 ms of seismic record below the sea floor. Sparker data allowed us to obtain enough penetration into the seafloor, even in sectors characterized by coarse-grained or consolidated sediments, providing a lateral resolution of 2.5 m and a vertical resolution of 1 m.

Furthermore, very high resolution seismic data were acquired using the Datasonic Chirp II operating at 3.5 kHz (2.5–7 kHz). Chirp data allowed for a greater spatial resolution (lateral resolution 0.6 m, vertical resolution 0.5 m), thus resolving more details in fine-grained superficial deposits. All seismic data were processed in order to increase the signal/noise ratio using the software Geosuite. Our interpretation of the seismic stratigraphy into seismic units was based on Mitchum et al. (1977).

3.3. Vibrocores, sediment analysis and shell sampling for radiocarbon dating

Three 3-meter-long sediment cores (V1, V2 and V5, Fig. 1), were collected using a vibrocorer mounted on the R/V Urania. The location of the cores was based on the analysis of seismic profiles in order to calibrate the shallow seismic units. The coordinates of the core positions were determined by the Differential GPS of the ship, whereas the depth of the seabed at each core sampling point was determined from the DTM.

Cores were immediately opened on board after their collection, they were described and dissected every 0.1 m, or in correspondence to a macroscopic change in sedimentary features. In the laboratory, sediment samples were dried at 60 °C, and sub-sampled by quartering for different analysis.

Gravelly sandy sediments were carefully washed with distilled water, and grain-size distribution was measured using dry sieving for the gravel/sand fraction between 4000 and 90 μm at half-phi intervals; the finer fraction (<90 μm) was analyzed using a Galai CIS 1 laser system at 5 μm intervals (Molinaroli et al., 2009). Sandy muddy sediments were treated with H_2O_2 in order to remove organic matter. They were then wet sieved at 90 μm. The coarser fraction (>90 μm) was analyzed using dry sieving between 2000 and 90 μm at half-phi intervals; the finer fraction (<90 μm) was analyzed using the Galai CIS 1 laser system. The core V1 was mainly composed of organic-enriched mud and the total organic matter was determined by Loss on Ignition, which measures the loss of weight after calcination at 500 °C for 3 h. For each sediment core, macroscopic shell samples were collected at different depth levels and classified in order to obtain additional information to discriminate between lagoon and marine depositional environments. Additional sediment data, available from De Falco et al. (2010), based on grab samples, were used for the calibration of the seismic units.

Four bivalve shell samples were collected from the three cores for radiocarbon dating. Articulated shells were only found and sampled at two levels of the core V1. Disarticulated shell samples were found and sampled from the other two cores. One sample was collected at a shell layer of the core V3 and one isolated shall sample was collected from the core V5.

3.4. Sea-flooding maps for 2100

The projected sea level rise rates and the related sea flooding scenarios of adjacent coastal sectors were analyzed in order to evaluate if the future evolution of present-day barrier–lagoon systems of the study area under conditions of accelerated sea-level rise can be compared to the evolution of the ancient analogue. A sea-flooding map was made based on 3 different scenarios of possible sea flooding expected for the year 2100.

The DTM (Digital Terrain Model) was obtained by joining different land and marine DTMs: 1) the coastline area, about 2 km wide, derived from Lidar data, with a spatial resolution of 1 × 1 m (http://www.sardegnageoportale.it/disclaimer.html); 2) the inland area derived from Shuttle Radar Topography Mission (SRTM) low-resolution data; 3) the shallow marine area derived from multibeam bathymetric data and 4) the deep sea area derived from the Gebco low-resolution bathymetric data.

The basic data derive from Church et al. (2013) (2013 IPCC report), assuming a CO_2 content of 700 ppm (projection 8.5) for which are represented the minimum and maximum flooding projections and the Rahmstorf (2007) model. For Church et al. (2013) the eustatic sea-level rise projection (due to thermostatic and eustatic effects) expected for 2100, shows a minimum and a maximum value of 53 and 97 cm respectively.

These reference values were inserted into a spreadsheet ("Vector project" http://vector.conismamibi.it/) which considers the isostatic and tectonic values calculated for the Oristano Plain. The isostasy values were derived from the Lambeck model (2011) published for Italy; the tectonic values were derived from the long and short term (MIS 5.5, late Holocene) bibliographic data (Ferranti et al., 2006; Orrù et al., 2011).

The map was created using the Global Mapper 13 software tool, "Generate contour"; the reference system used was UTM, WGS84, Zone 32.

4. Results

4.1. Morphological features of drowned barriers and direct observations of the seabed

A three-dimensional view of the Digital Terrain Model of the marine sector studied is reported in Fig. 2 (see Fig. 1 for the location of the DTM on the map). The deepest offshore sector, to the west, and inner sector inside the Gulf of Oristano, to the east, are characterized by a low gradient seafloor, with slope ranging between 0 to 0.2°. The undulated morphology in the inner sector of the DTM is associated with the presence of

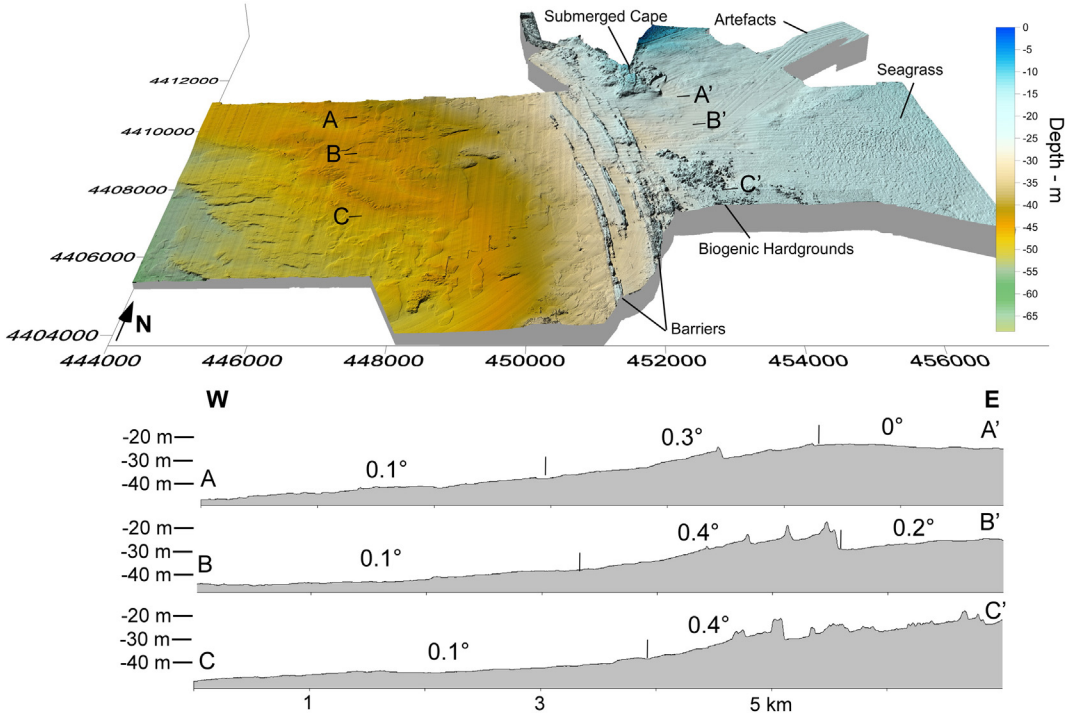

Fig. 2. Three-dimensional view of the seabed with drowned barriers. In the lower part, bathymetric profiles with the seabed gradient values.

seagrass meadows, whereas the more irregular morphologies are associated with the offshore prolongation of the northern cape of the gulf to the north, and to the presence of hardground formed by bio-constructions mainly composed by calcified red algae to the south (De Falco et al., 2010).

The outer and inner sectors are connected by a more sloping seafloor (0.3°–0.4°) where several elongated ridges occur. These ridges form a sequence of parallel and discontinuous forms in relief, in a depth range of 18–37 m (Fig. 3). The deeper ridge (Br 1, Fig. 3), is only visible in a limited sector of the study area, at 35.7–37.3 m of depth (considering the top and the offshore base of the ridge) and is elevated 1.6 m above the seafloor. A series of ridges (Br 2, Fig. 3) is located in the depth range of 24.5–29.2 m. These ridges represent two distinct series of elongated shapes (Br 2a and Br 2b), the former located at 26.7–29.2 m, the latter at 24.7–26.8 m of depth. Their elevation is up to 2.5 m above the seafloor and, in some sectors, have a double crest on the top (Fig. 3, Profile C). The third series of ridges is located at a depth of 17.8–24.2 m (Br 3, Fig. 3). In this case there are also two main series of elongated forms (Br 3a and Br 3b, 17.8–22.9 m and 19.6–24.2 m deep respectively), which are elevated up to 5.1 m above the seabed. However, minor ridge traces are visible in the spaces between the main ridges in different sites, and the inner ridge (Br 3b) is characterized by two well-separated crests (Fig. 3).

The elevation of the ridges above the seabed increases from the offshore ridges (Br 1) to the inshore ridges (Br 3) and range from 1.6 m up to 5.1 m, when considering the drop between the top of the ridge and the seabed offshore. The cross profiles show that, in some cases, the drop between the crest and adjacent landward depression is as much as 10 m (Fig. 3, profile B, ridge Br3b).

The scuba dive inspection of the inner ridge (see Fig. 3 for the location of the dive point), revealed that it was covered by a hardground formed by slabs of fractured conglomerates (Fig. 4 a–d), colonized on the crest by a biogenic hardground (Fig. 4e) covered by seagrass (Fig. 4b). The conglomerates (Fig. 4f) overlie unconsolidated fine sands (Fig. 4e), whereas medium-fine biogenic sands were found between the two barrier crests. ROV inspection revealed that the back-barrier sector was floored by a rippled sedimentary seafloor, with a wavelength of about 1 m, with crests parallel to the direction of barrier orientation.

4.2. Seismic stratigraphy

The analysis of seismic reflection profiles allows us to identify the nine seismic units described in Table 1. The seismic units were defined on the basis of their external form, upper and lower boundaries (when it is visible) and typical reflector configuration.

The seismic unit Ua is most prominent in the offshore portion of the seismic profiles and is marked by an abrupt lateral termination below the ridges. It is the basal unit; its base is masked by multiple reflections and its internal configuration is characterized by low-amplitude parallel reflectors, erosionally truncated at their upper contacts (Figs. 5 and 6). Ub is observed inshore, landward of the ridges. It is characterized by wavy, discontinuous and low-amplitude reflectors that are erosionally truncated at the top of the package (Figs. 6 and 7). The base is masked by multiple reflections. Ub and the Ua are in lateral contact and are separated by a subaerial unconformity. Uc was observed beneath and to seaward of the ridges (Figs. 5 and 6). It is characterized by high-amplitude sigmoid and parallel reflectors, that downlap the lower boundary over the Ua and Ub units. In comparison, the upper boundary is an erosional truncation. The thickness of this unit reaches 15 ms in the ridge sector.

The Ua, Ub and Uc units are truncated by a subaerial unconformity which has been represented as dashed red lines in Figs. 5, 6 and 7.

U1 infills a depression incised into the Ua and Uc units in the offshore (Fig. 5). Medium amplitude reflectors, with wavy clinoform configurations, downlap and onlap the lower boundary. The upper boundary is concordant with the upper-most reflectors. The thickness ranges between 3 ms and 20 ms. U2 is limited to the ridge substrate and typically does not show a clear reflector pattern (Fig. 6). However, occasional convex upward reflectors can be observed (Line 2, Fig. 6). This unit is generally opaque due to the poor penetration of the seismic waves below the cemented ridges and the lower boundary is not visible. U3 infills the adjacent landward depression (Fig. 7). This seismic unit was divided into two sub-units (U3a and U3b). U3a is characterized

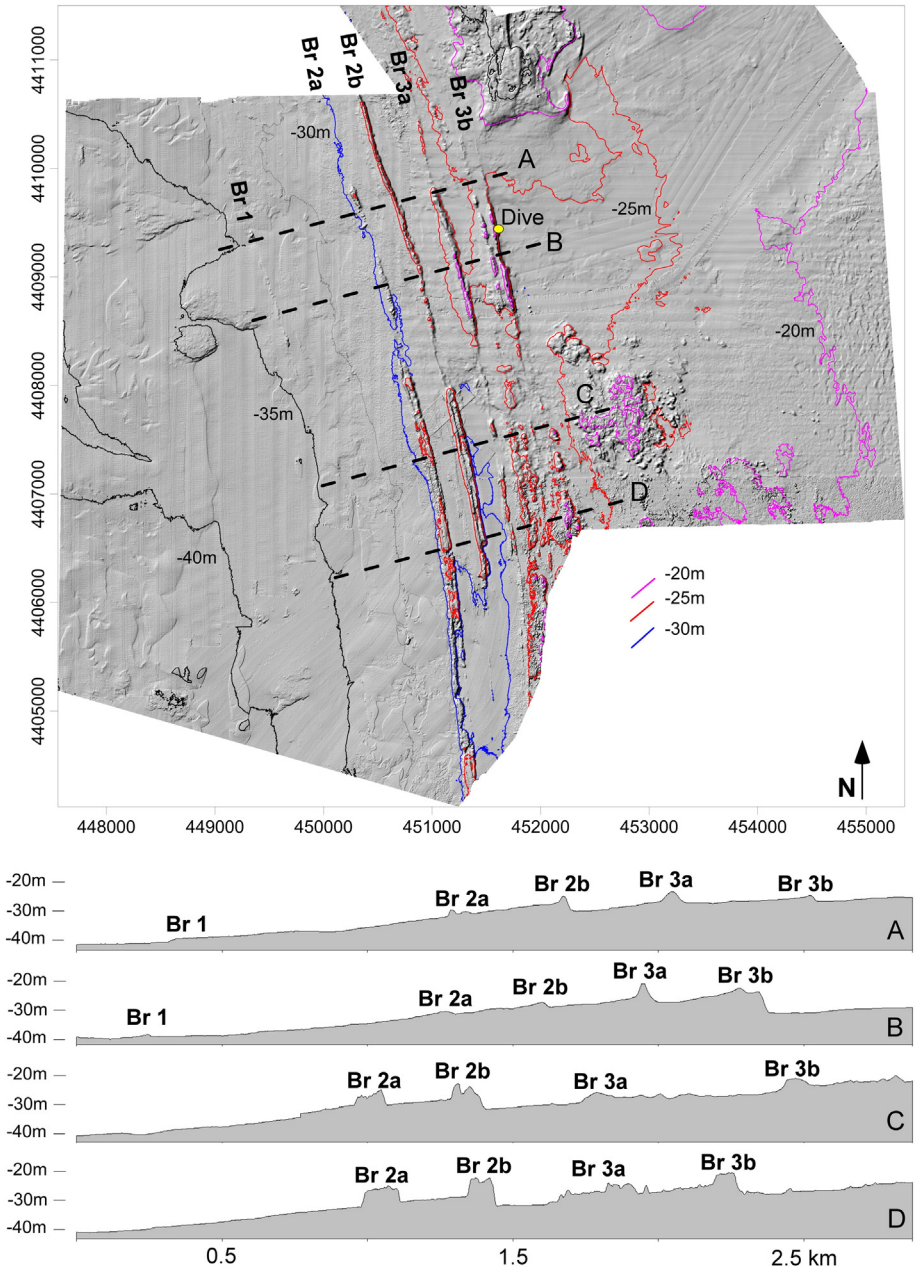

Fig. 3. Digital Terrain Model showing the barrier morphology and depth contour lines. In the lower part, cross bathymetric profiles of the barriers.

by continuous parallel internal reflectors, U3b by sigmoid prograding internal reflectors. U3 reflectors onlap the lower boundary and toplap with the upper boundary. The maximum thickness of U3 is 18 ms.

U4 is characterized by prograding, high-amplitude reflectors. These reflectors downlap the lower boundary and toplap with the upper boundary. This unit is up to 10 ms thick and overlies the Ub units and is in lateral contact with the U3 unit.

U5 occurs immediately to landward of the ridges, in the adjacent depression (Fig. 7). U5 has a series of landward prograding, medium-amplitude reflectors. Reflectors onlap the lower boundary while they are erosionally truncated in the upper boundary. This unit overlies the U3a and is onlapped by the U3b and U6 units. The maximum thickness is 10 ms (Fig. 7).

U6 represents a surficial drape with continuous parallel reflectors and overly the wave ravinement surface (WRS). This unit has limited thickness, often it is thinner than the vertical resolution of the sparker profiles. In such cases the unit is only visible in the Chirp sections.

4.3. Lithofacies and calibration of seismic units

For the calibration of the seismic unit Ua, we refer to a previous study (Francolini et al., 1990) which reported the description of the stratigraphy of three cores collected to the north of the study area. The cited authors sampled a marine lithofacies composed of clay sediments which they dated early Pliocene, based on the micropaleontological content. This lithofacies was correlated with a seismic facies, called Unit C, found in the shelf sector just outside of the Gulf of Oristano (Lecca, 2000). The Ua seismic unit can be correlated to Unit C (Francolini et al., 1990; Lecca, 2000) based on the comparison of our seismic records with those reported by the cited authors and are thus attributed to the marine deposits of the early Pliocene. The seismic

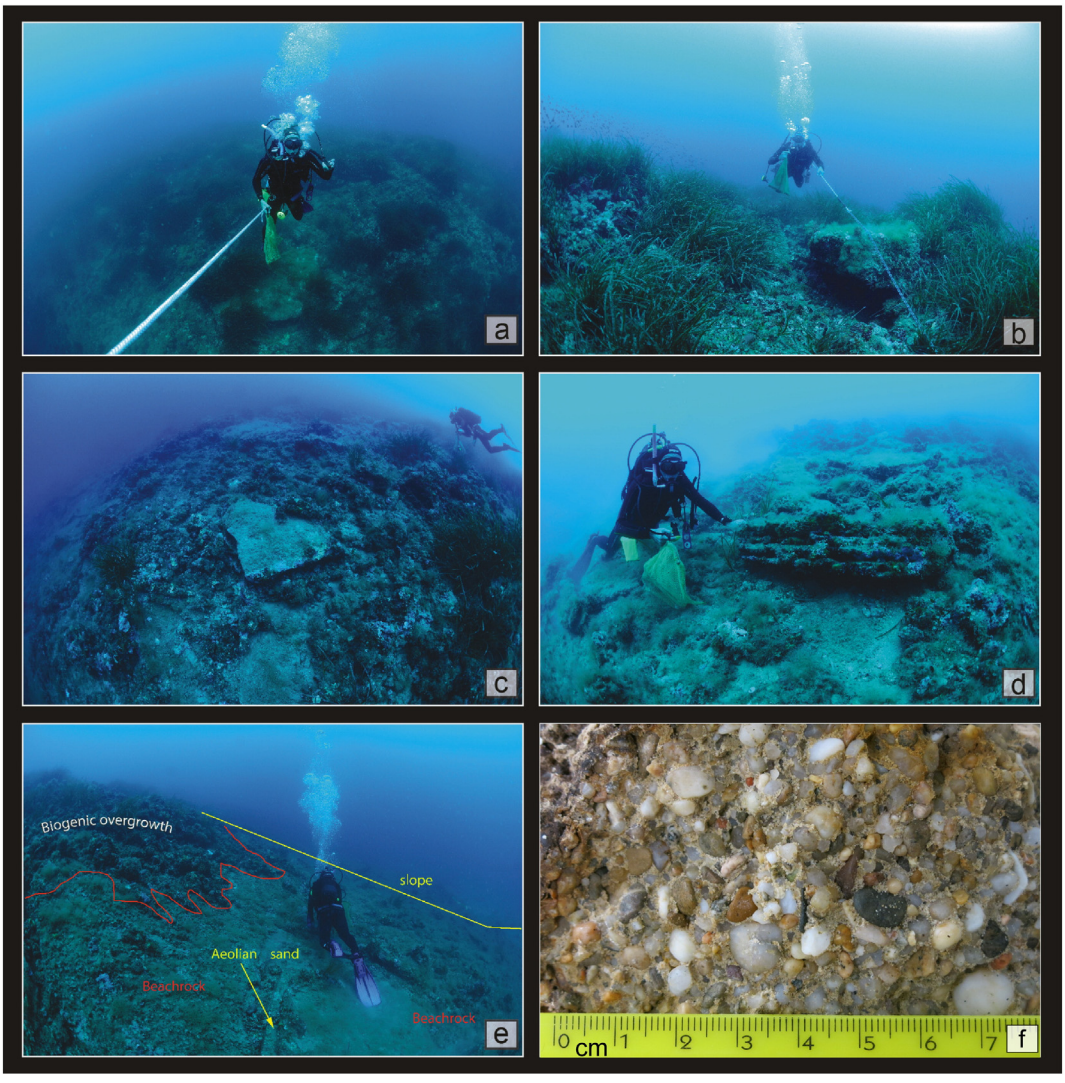

Fig. 4. Panel of barrier images. a: 5 m on the top of the submerged barrier, the strong marine tide enhanced by the anchor rope angulation. b: On the top of the barrier, −18 m. c: An overview of the barrier top with the broken beachrock boulders. d: A stratified beachrock boulder. e: The barrier profile showing the slope inward of the Gulf of Oristano, −27 m. f: Conglomerate sample (see Fig. 3 for the location of the dive point).

units Ub and Uc were not calibrated, but they can be considered pre-Holocene as they are truncated by the subaerial unconformity.

The three cores (V1, V2 and V5, Figs. 1 and 8) sampled the seismic units U1, U3, U4 and U6. The depth levels used for the description of the down-core profiles (Fig. 8) refer to the present-day mean sea level.

V2 was collected seaward of the ridges, at a depth of 39 m, and sampled the incision which cut Ua (Fig. 5). The grain-size profile along the core shows the prevalence of medium-fine sands for an interval of 2.7 m, with the exception of two horizons with coarser grain sizes (the upper level at 39.0–39.1 m and the level between 39.8 and 40.1 m, Fig. 8). Sediments of this core portion are composed of mixed siliciclastic and bioclastic sands with a paleontological content composed of echinoids, bryozoans and bivalves of marine environments. This core portion is correlated to the U6 seismic units.

A shell layer, composed of coarse bivalves and gastropods, marks an abrupt change in sediment texture at 41.6 m, corresponding to the

Table 1
Description of seismic units interpreted from the seismic reflection profiles.

Seismic units	Geometry	Upper boundaries	Lower boundaries	Reflector configuration
Ua	Base unit	Erosional truncation	//	Parallel, top discordant, low amplitude
Ub	Base unit	Erosional truncation	//	Wavy, discontinuous, low amplitude
Uc	Wedge	Erosional truncation	Downlap	Sigmoid/parallel, continuous, high amplitude
U1	Fill	Concordance	Onlap/downlap	Hummocky clinoforms, continuous, medium amplitude
U2	Mound	//	//	No stratal pattern
U3	Fill	Concordance/toplap	Onlap	Parallel/sigmoid, continuous, high amplitude
U4	Sheet/wedge	Toplap	Downlap	Prograding parallel/sigmoid oblique, continuous, high amplitude
U5	Bank	Toplap/no strata	Onlap/no strata	Prograding parallel/sigmoid oblique, continuous, medium amplitude
U6	Drape	//	Concordance/onlap	Parallel, continuous, high amplitude

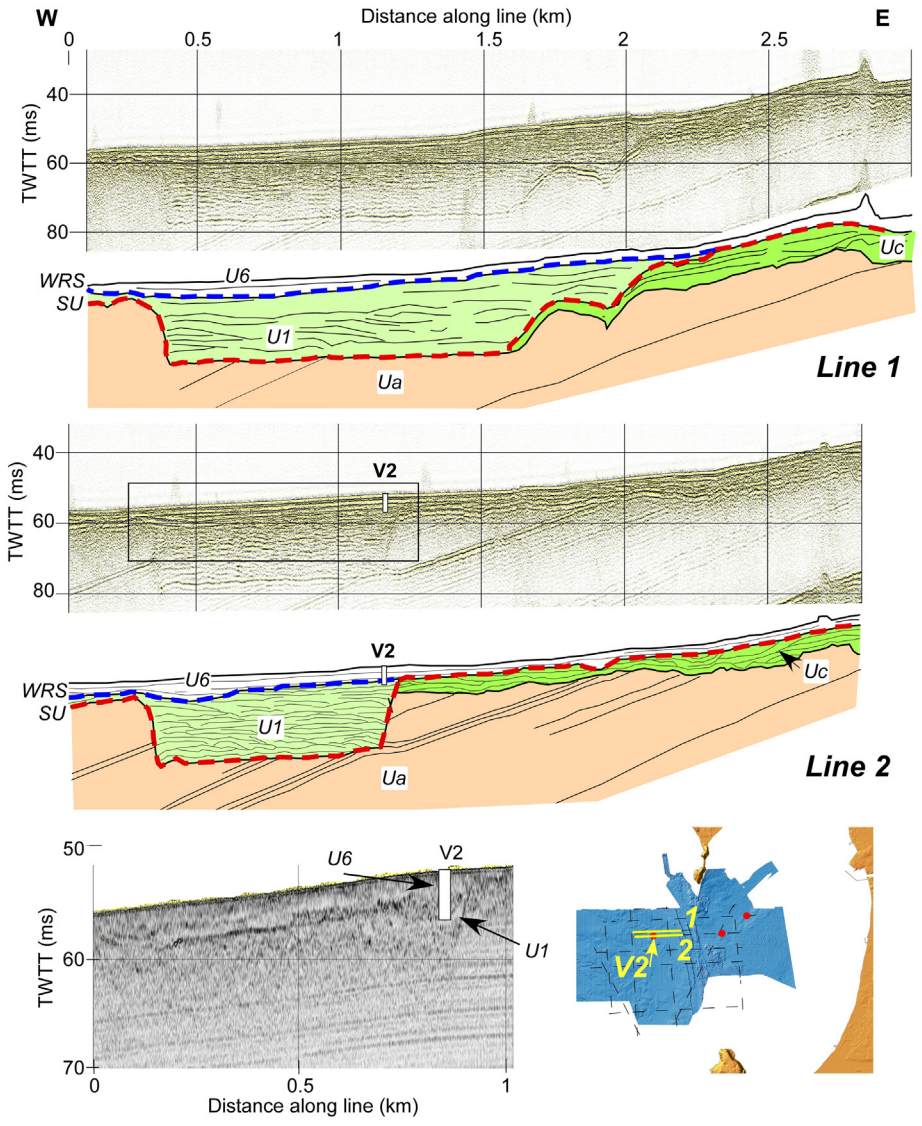

Fig. 5. Raw and interpreted high resolution seismic profiles (sparker source) of the sector offshore the barriers. The location of the vibrocore V2 along the Line B is reported. In the lower part: very high resolution seismic profile (Chirp) of the sector of the core sampling. (For interpretation of the reference to color in this figure, the reader is referred to the web version of this article.)

boundary separating seismic units U6 from U1. The lower part of the core is composed of well rounded pebbles, mainly comprising metamorphic rocks, supported by a sandy–gravelly matrix. The grain size reported in the deeper portion of the core profile refers to the matrix (Fig. 8). This boundary correlates to the WRS (Fig. 5, line 2).

V1 was collected in the landward depression from a depth of 25 m (Figs. 7 and 8). The upper 0.3 m (25.0–25.3 m) were composed of gravelly sands, again corresponding to the U6 unit. This layer overlies organic-rich muddy sediments which were correlated to the U3 unit. From 25.3 to 26.3 m this lithofacies was composed of sandy muds (25%–49% of sand) with 4–11% of organic matter (U3b). From 26.3 to 27.4 m the sand content decreased (4%–18%), with 9%–14% of organic matter (U3a). Medium-fine sand increased downward (27.4–28 m) becoming predominant in the lower portion of the core. The paleontological content was characterized by the dominance of a bivalve (*Loripes* sp.) which was found to be associated with *Dentalium* sp. in the upper U3b unit (25.4 m). This forms a layer of well-preserved shells, many of which are still articulated, at the core base (28 m).

Core V5 was collected at a depth of 23 m, inshore from core V1. The surficial layer, 0.4 m thick (23.0–23.4 m), was composed of gravelly sands mixed with seagrass litter (U6). Down-core (U4), a layer 1.3 m thick (23.4–24.7 m) of terrigenous granules and pebbles with a sandy matrix was found. This lithofacies contains small bivalves. An abrupt change of sediment texture occurred at 24.7 m where sediments became finer, mainly composed of medium-fine sands. The paleontological content in the deeper portion of the core (24.7–26 m) was characterized by the presence of bivalves and echinoids of the marine environment.

U2 can be correlated with the conglomerate sampled by divers over the cemented ridges (Fig. 4), and comprised siliciclastic and lithic granules weakly cemented by carbonate. The U5 unit was not calibrated with a sediment sample. The U6 unit was further characterized by grab samples (De Falco et al., 2010) and was composed of mixed bioclastic/siliciclastic medium sands and siliciclastic sandy gravels.

4.4. Radiocarbon data and vertical tectonic movements

Four fossil shells collected from the three vibrocores were sampled and dated using radiocarbon techniques in order to infer an age model of the system (Table 2 and Fig. 9). Two samples (13V1 and 14V1, Table 2) were collected from core V1 (Fig. 8), corresponding to the U3 unit and were dated at 8674 ± 105 and 9490 ± 69 calibrated years

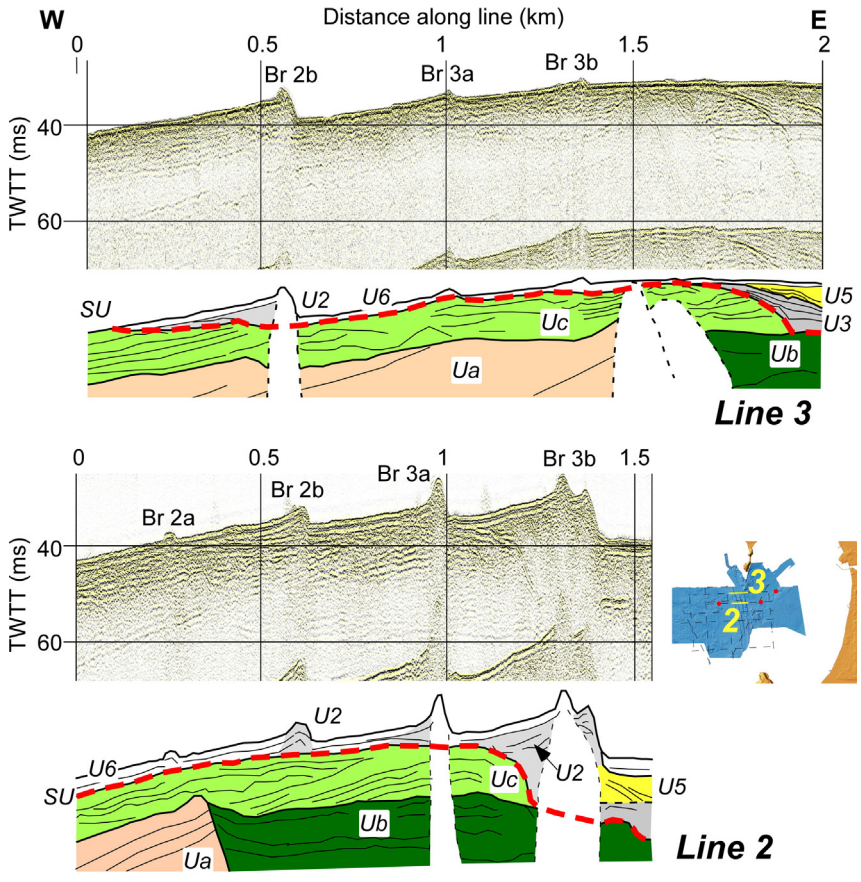

Fig. 6. Raw and interpreted high resolution seismic profiles (sparker source) of the sector of the barriers. (For interpretation of the reference to color in this figure, the reader is referred to the web version of this article.)

BP. Both samples were shells of the lagoonal specimen *Loripes lacteus*, and they were collected at a depth downcore of 25.7 m and 28 m below the present sea level (Fig. 8). These lagoonal samples were considered to have not been reworked after their burial because they were still articulated. The former value agrees with the predicted values (Fig. 9 and Table 2, Lambeck et al., 2011) The latter value is above the sea level curve: this could be related to the altitude error associated with the sea level marker (Lambeck et al., 2004).

Two other samples (16V2 and 19V5) were collected from cores V5 and V2 respectively. The latter sample (16V2, *Cardium* sp.) was collected in order to date the shell layer between U1 and U6 at a depth downcore of 41.6 m, at the level corresponding to the WRS (Fig. 7). The age was 7610 ± 89 calibrate years (Table 2).

The former sample (19V5, *Ostrea* sp.) was collected in order to date the U4 unit at a depth downcore of −25.8 m (Fig. 7). The calibrated age was 7094 ± 112 y (Table 2).

4.5. Depositional environments

The interpretation of the depositional environments of each seismic unit identified is based on the lithological information derived from vibrocores, grab samples, direct inspections and previous studies (Table 3). Three seismic units were not calibrated due to the absence of sediment samples. Their depositional environments were inferred by their stratigraphic pattern.

Ua, Ub and Uc represent the basal units. Ua is composed of fine grained marine deposits of the early Pliocene (Francolini et al., 1990; Lecca, 2000). This unit is not present in the Gulf of Oristano because it deepens along the main fault of the Campidano graben (Fig. 1).

These three basal units are truncated by the subaerial unconformity, which represents a surface of erosion (or no deposition) created during a lowering of the sea level presumably during the last glacial maximum by subaerial processes (Catuneanu, 2006).

In the offshore sector, a 15–20 m deep incised valley, which is delimited by the subaerial unconformity, is filled by U1, of which the top is composed of matrix-supported pebbles and cobbles, which can be interpreted as alluvial deposits. These alluvial deposits filled the river valley during the initial phases of the last rise of the sea level (before 7610 calibrated years BP as inferred from the ^{14}C sample 16V2). The U1 is limited upwards by the Wave Ravinement Surface (WRS) which separates marine (U6) and continental (U1) deposits. The U2 is composed of gravelly, siliciclastic sediments weakly cemented by carbonates. We interpret these beachrocks to represent the paleo-barrier islands, particularly the crest and shore sector of the barrier–lagoon system. Beachrocks are hard coastal sedimentary formations consisting of beach sediments, rapidly cemented by the precipitation of carbonate cements. Lithification usually takes place in the intertidal zone (Vousdoukas et al., 2007, and reference therein). In our case lithification occurred for the whole barrier crest, from the barrier shore to the backshore face of the ridge.

U3 consists of fine-grained, organic-rich sediments which were deposited in a backbarrier depositional environment. U3a overlies the pre-Holocene deposits (Ub) and is in lateral contact with the U4 unit. This subunit is composed of organic silt and clay sediments that represent the infilling of the back-barrier–lagoon in a very sheltered environment, when sea level was too low for washover to occur. Sub-unit U3a occurs between 52 ms and 39 ms (corresponding to −39 m and −29 m respectively). Upwards, U3b has a sandier composition (as seen in core V1) and is laterally in contact with U5. The latter unit is

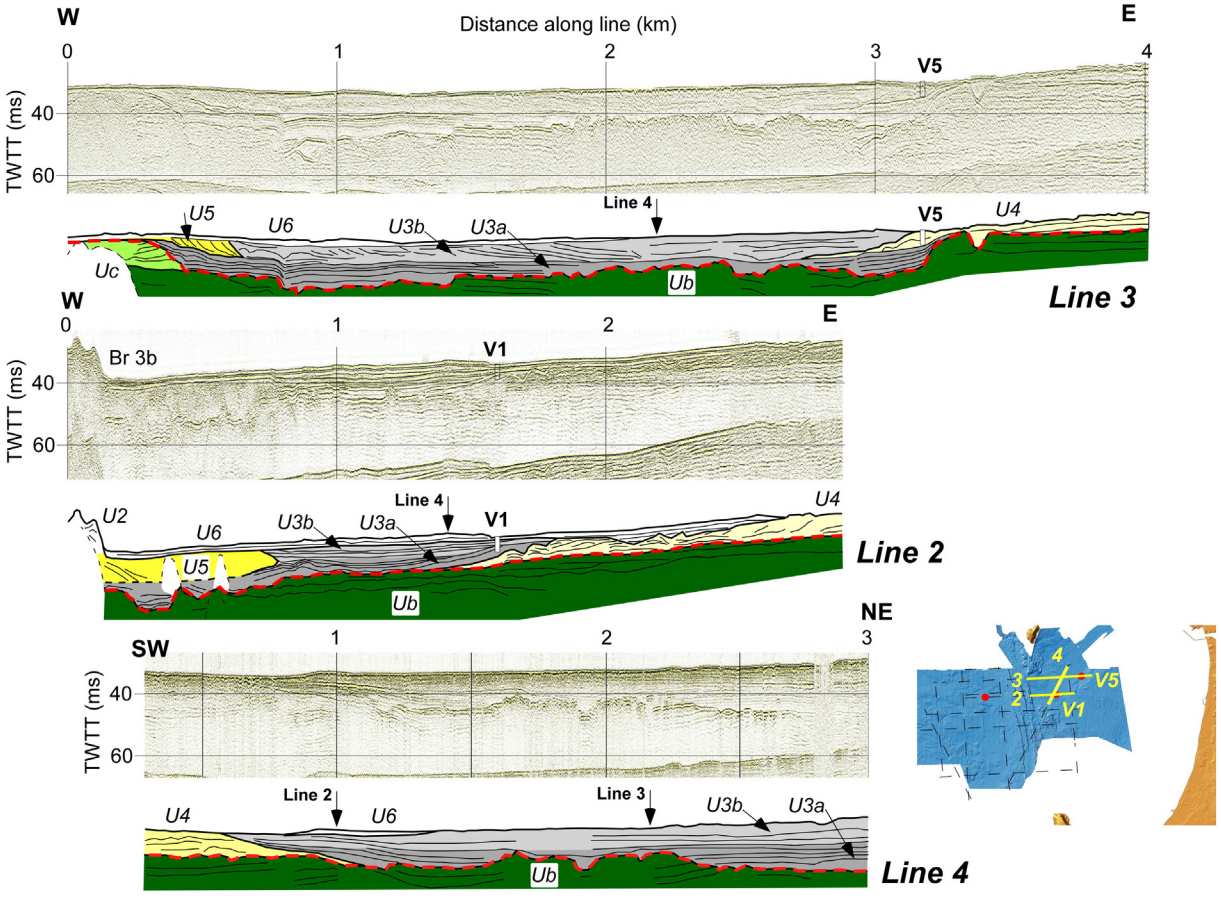

Fig. 7. Raw and interpreted high resolution seismic profiles (sparker source) of the back-barrier region. The locations of the vibrocores V1 and V5 along the Line B and Line C are reported. (For interpretation of the reference to color in this figure, the reader is referred to the web version of this article.)

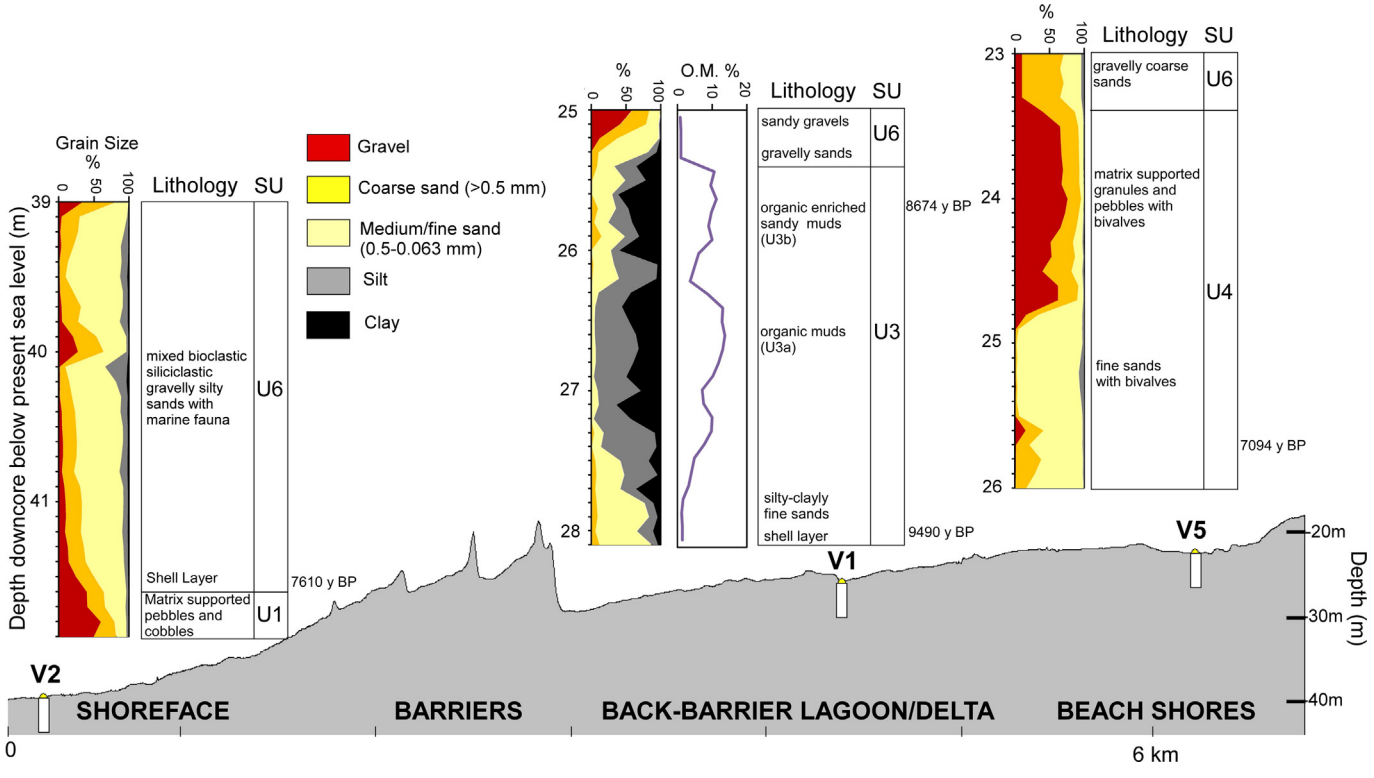

Fig. 8. Along-core sediment grain size and sedimentary facies description. The associated seismic units are also reported. The along-core organic matter content is reported for the core V1.

Table 2
Radiocarbon data (CEDAD University of Lecce, Italy) and calibrated ages using Calib 7.02 program.
Stuiver et al. (2014)

Sample ID/vibrocore	Kind of shell	Radiocarbon age Years	$\delta^{13}C$ (‰)	Calibrated age Years	Altitude m	Predicted 2011 m	Predicted 2004 m
13V1	*Loripes lacteus*	8192 ± 45	−5.7 ± 0.7	8674 ± 105	−25.7	−25.4	−28.5
14V1	*Loripes lacteus*	8834 ± 45	−0.6 ± 0.4	9490 ± 69	−28	−39	−36
19V5	*Ostrea* sp.	6570 ± 35	−0.4 ± 0.1	7094 ± 112	−25.8	−12	−13
16V2	*Cardium* sp.	7130 ± 50	−2.3 ± 0.3	7610 ± 89	−41.6	−17	−18

Altitude is the sum of water depth below the present sea level and downcore depth (see Fig. 8). Altitude of the predicted sea level was estimated using the Lambeck et al. (2004) and Lambeck et al. (2011) models.

located in the back-barrier region and is characterized by a prograding reflector pattern which we attribute to washover processes (Shan et al., in press). U3b represents the infilling of the back-barrier–lagoon in more high energy conditions, with storm waves capable of overwashing the landward barrier crest. This interpretation is further supported by the coarsening upward of V1 core (Fig. 8).

U4 is composed of fine sands to matrix-supported granules and pebbles, and is located in the landward sector of the back-barrier basin. The stratigraphic pattern is characterized by a seaward prograding parallel/sigmoid reflector configuration. These features lead us to consider U4 as beach deposits of the inner shore of the back-barrier basin. The upward coarsening along the core V5 at 24.8 m of depth could be related to the prograding shoreline as the lagoon/backbarrier segmented and it shallows. U6 represents the present-day marine sediments formed by the winnowing by waves of previous sediments or by carbonate sediments of marine origin.

The morphology of the antecedent topography of the barrier system in the Gulf of Oristano, obtained by interpolation of the subaerial unconformity surface which cuts the basal Units (Ua, Ub and Uc), is reported in Fig. 10A. A large channel crosses the barrier region which can be interpreted as the incision made by the Tirso river valley during the last decline in sea level over the three basal units Ua, Ub and Uc (Schumm, 1993). The total thickness of the sediment deposited following the last sea-level rise (U1 to U6 units) is reported in Fig. 10B. Two main depocenters can be identified: (i) on the offshore side from the barriers (B) the late Pleistocene–Holocene deposits are mainly represented by the alluvial infill (U1) of the river valley (Figs. 5 and 10) following the decrease of competence of the river and (ii) on the inshore side of the barriers (A) the transgressive back-barrier deposits (U3, U4 and U5) filled the river valley (Figs. 7 and 10).

4.6. Flooding of the present day barrier–lagoon system

The sea-level rise expected for the year 2100 is the result of modeling that takes into account the isostatic and tectonic values calculated for the Oristano sector. These are −0.62 mm y^{-1} and 0 mm y^{-1} respectively (Ferranti et al., 2006; Orrù et al., 2011). This is in addition to the estimated predictions of eustatic sea-level rise. Two cases are considered (i) 53 and 97 cm (the minimum and maximum values respectively) according to the 2013 IPCC projections, and (ii) 140 cm according to the 2007 Rahmstorf projections.

From this modeling three possible values corresponding to the sea-level altitude for the year 2100 are derived: 54.4 cm and 94.9 cm (the minimum and the maximum according to the Church et al., 2013 projection) and 134.5 cm (the maximum according to the 2007 Rahmstorf projections).

These values correspond to a sea level rise rate of 6–15 mm y^{-1} which is similar to the sea level rise rate which occurred during the barrier–lagoon system formation (10–15 mm y^{-1}, Lambeck et al., 2004, 2011).

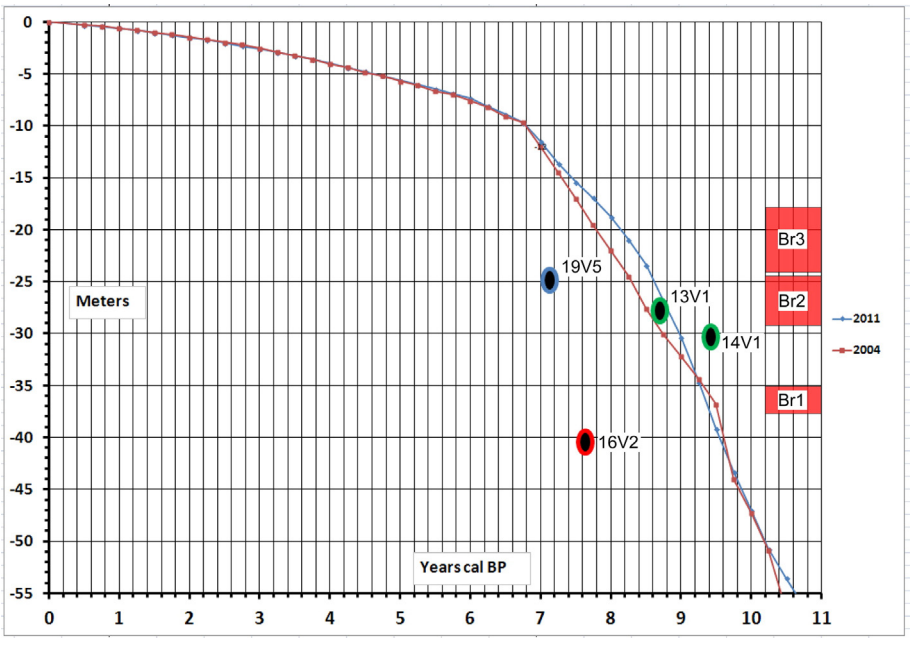

Fig. 9. Predicted sea-level curves of the Lambeck model (in red 2004, in blue 2011) calculated for the Gulf of Oristano. Green–black balloon: vibrocore 1 samples. Red–black balloon vibrocore 2 samples. Blue–black balloon vibrocore 5 samples. The depth of the barriers Br1, Br2 and Br3 is reported. (For interpretation of the references to colors in this figure legend, the reader is referred to the web version of this article.)

Table 3
Depositional environments associated with the seismic units interpreted through their correlation with lithofacies and stratigraphic patterns.

Seismic units	Calibration	Lithofacies	Interpretation
Ua	Core (Francolini et al., 1990)	Mud	Early Pliocene
Ub	No data	No data	Alluvial deposits (Pleistocene)
Uc	No data	No data	Alluvial/Aeolian deposits (Pleistocene)
U1	Vibrocore V2	Matrix supported pebbles and cobbles	River valley infill during transgression
U2	Direct sampling by scuba diving	Cemented gravelly sand	Beach-rock/barriers
U3	Vibrocore V1 and grab samples	Organic-rich mud to sandy mud	Back-barrier deltaic/lagoonal deposits
U4	Vibrocore V5	Fine sands to matrix supported granules and pebbles	Beach shore deposits of the back-barrier basin
U5	No data	No data	Overwash deposits
U6	Vibrocore V1, V2, V5 and grab samples	Sand to gravel	Present day shoreface deposits

The passive flooding map of the Oristano Plain, based on this projection, is reconstructed on the high resolution DTM (Fig. 11a); this shows the possible areas which could be subject to coastal flooding. Two present day barrier–lagoon systems will be drowned following sea level rise: the Mistras lagoon at north and the Corru S'Ittiri lagoon at south.

Particularly, the maximum projections for the rise in sea-level (134.5 cm equivalent to a sea level rise rate of 16 mm y^{-1}), would cause the drowning of the barrier of the Mistras barrier–lagoon system (Fig. 11b1–b4).

5. Discussion

The barrier complex of the Gulf of Oristano is a case of barrier retreat through overstepping whose formation, evolution and preservation presumably were controlled by the inherited topography and the early barrier cementation.

The likelihood of preservation of barrier systems through overstepping depends on several factors. High sea-level rise rates favor barrier preservation (i.e. 60 mm y^{-1}, Storms et al., 2008) and deeper preserved systems (60 m and 100 m of water depth, South Africa, Salzmann et al., 2013; Green et al., 2014; 80 m/90 m South Adriatic, Storms et al., 2008), have been associated with meltwater pulses of the early phase of the last sea-level rise. Zecchin et al. (2015) have also recently shown a drowned delta at shallow depth which could be associated with a rapid increase of the sea level rise rate at shallow depth.

The rate of sea-level rise during the evolution of the barriers in the Gulf of Oristano can be estimated at 10–15 mm y^{-1} according to the sea-level curves (Lambeck et al., 2004, 2011) shown in Fig. 9. This rate is similar to the one reported by Storms et al. (2008), for the overstepping systems of the North Adriatic (10 mm y^{-1}, −40 m of depth). The same authors highlighted that this relatively low rate of sea-level rise should be in contrast with barrier preservation and that other factors (i.e. antecedent topography), may be of primary importance in barrier evolution (Mellett et al., 2012; Green et al., 2013; Lorenzo-Trueba and Ashton, 2014).

The landscape evolution of the barrier–lagoon system of the Gulf of Oristano is represented in Fig. 12. The first phase is the formation of a carved-out valley related to the sea-level decline of the Last Glacial Maximum (Fig. 12A). The presence and the role of paleovalleys have also been reported for other sites (Mellett et al., 2012; Green et al., 2013): they were considered a conduit for sediment transport during sea-level lowstand and subjected to backstepping infilling during transgression. In our case, the paleovalley of the Tirso river created the accommodation space for the sediment deposition. The sea-level rise allowed for the infilling of the paleovalley with alluvial deposits in the seaward

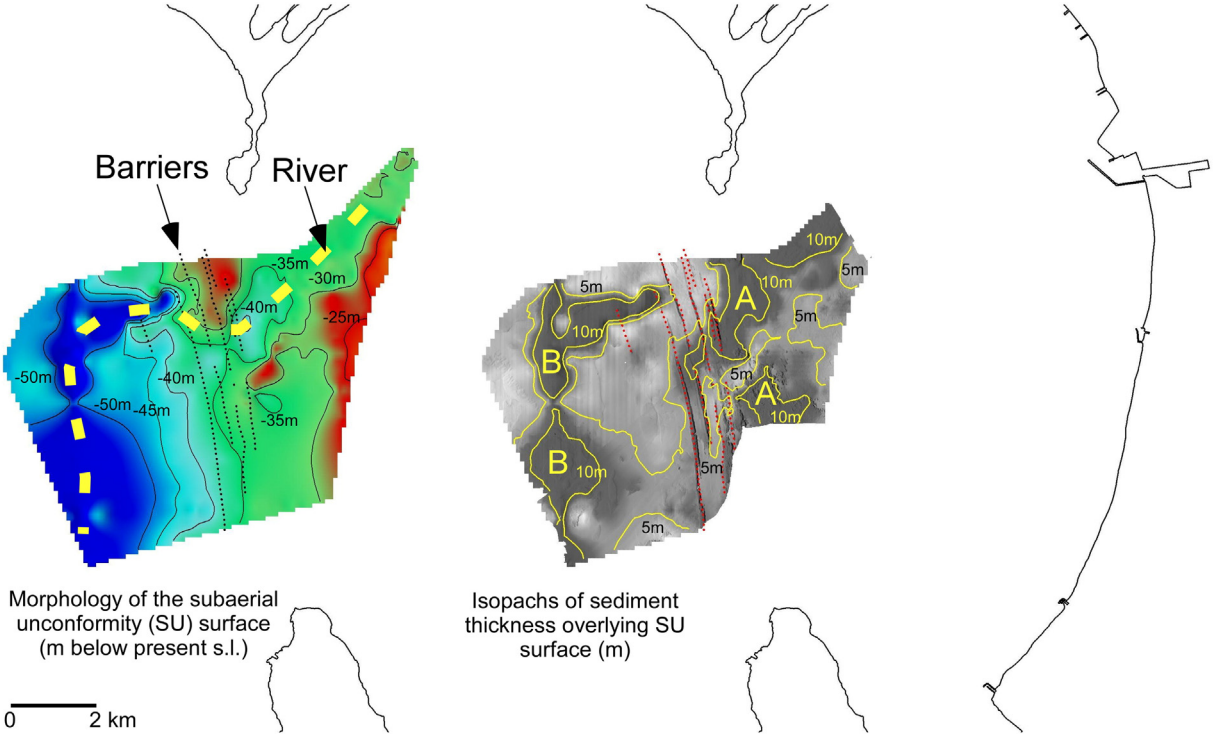

Fig. 10. A) Morphology of the topography antecedent to the last rise in sea level. B) Thickness of sediments deposited during and after the last rise in sea level.

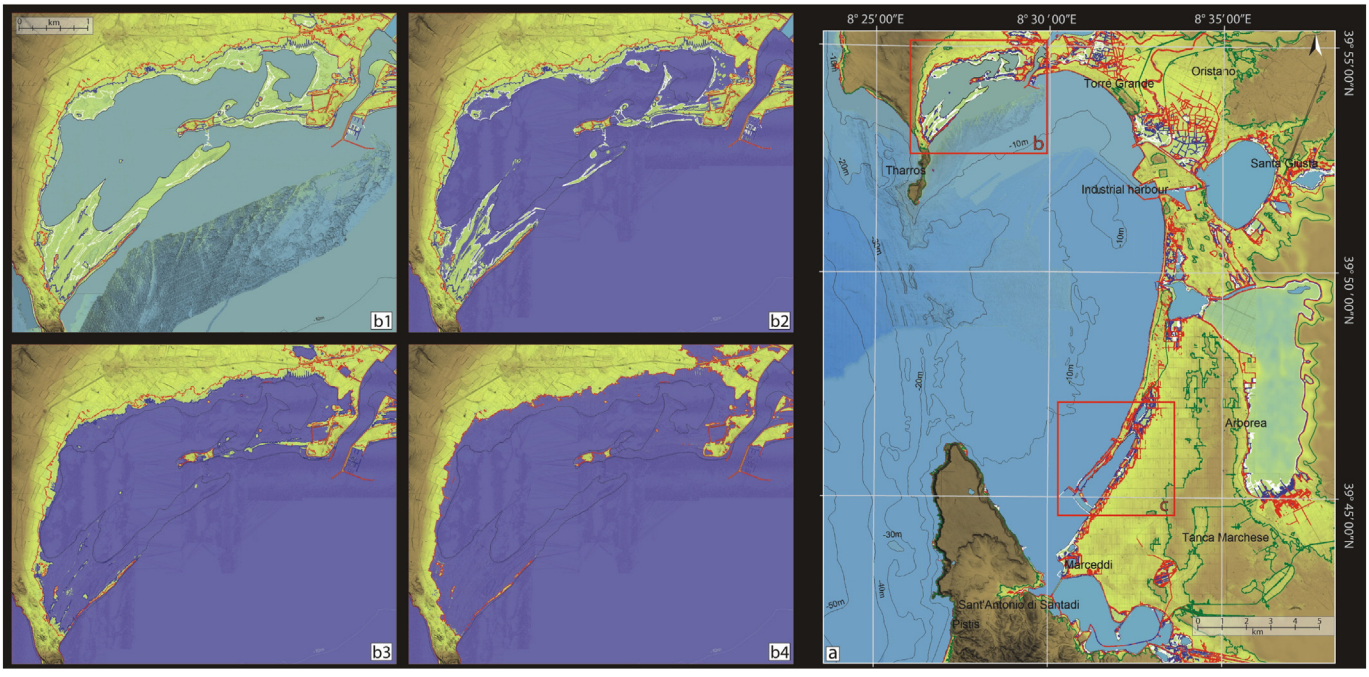

Fig. 11. Sea-flooding map of the Oristano plain expected for the year 2100 according to the Church et al. (2013) (2013 IPCC report) minimum projection (white line), Church et al. (2013) maximum projection (blue line) and Rahmstorf (2007) maximum projection (red line); contour line +5 m (green line) (a). Mistral lagoon (b); Corru S'Ittiri lagoon (c). Sea flooding map zoom of Mistral lagoon (b1); sea flooding modeling according to the Church et al. (2013) minimum projection (b2); sea flooding modeling according to the Church et al. (2013) maximum projection (b3) and sea flooding modeling according to the Rahmstorf (2007) maximum projection (b4). (For interpretation of the references to colors in this figure legend, the reader is referred to the web version of this article.)

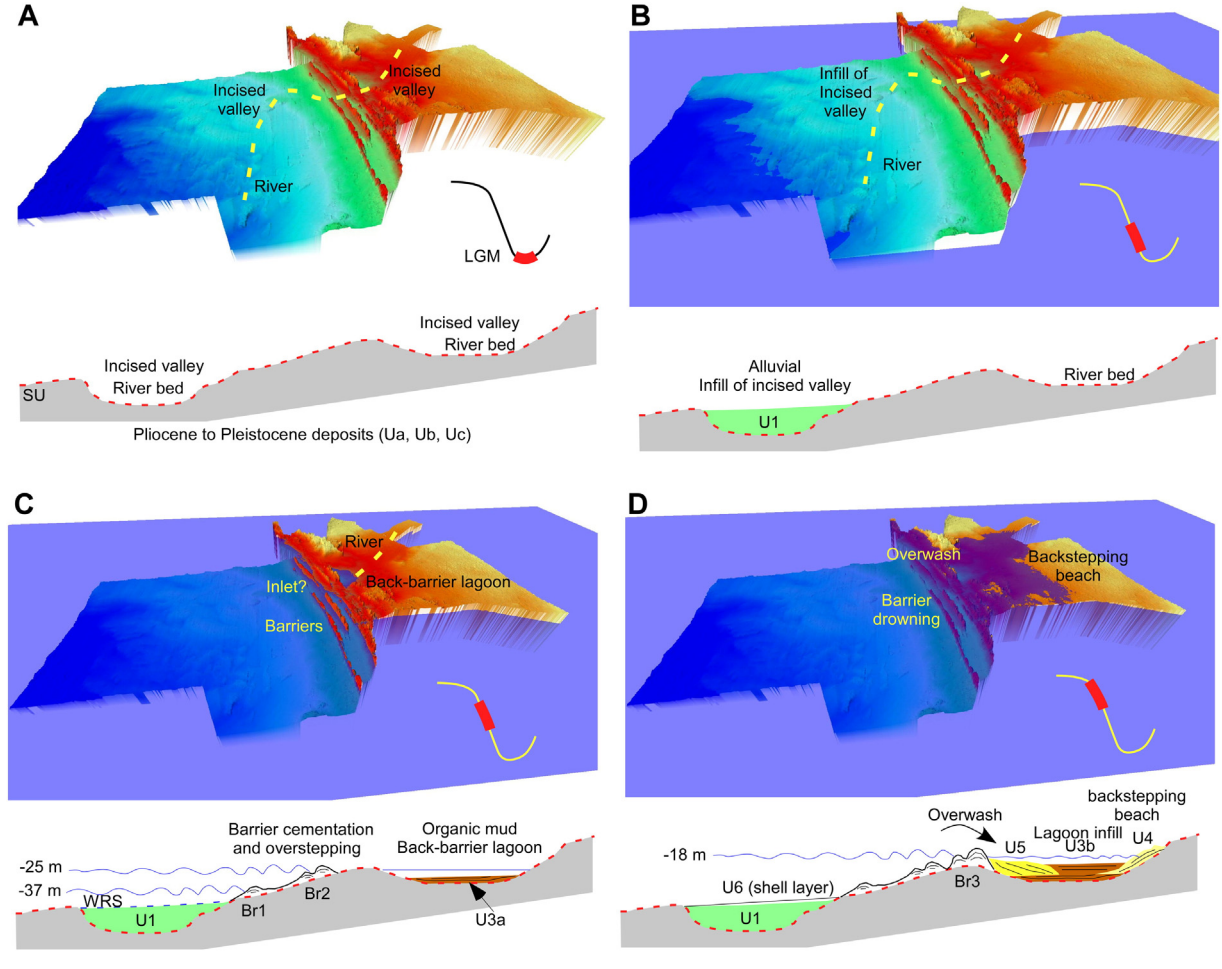

Fig. 12. Evolutionary model of the barrier–lagoon system of the Gulf of Oristano following the last sea-level rise (see Tables 1 and 3 for seismic unit description and interpretation).

sector of the alluvial plane, on the offshore side of the barrier, following the decrease in competence of the river (Fig. 12 B).

The marine transgression in the offshore side of the barrier occurred along a sub-planar surface with a gradient of 0.1° (slope 0.0017). During this phase, wave erosion along the ravinement surface prevailed in the shoreface, and the sediment supplied by the river was reworked by longshore currents forming the barrier islands. The barrier formation and overstepping are associated with an increase in the seabed gradient (0.3°–0.4° equivalent to 0.005–0.007). The increase in the seabed slope is generally associated with the barrier retreat under dynamic equilibrium, whereas barrier drowning is more likely for flatter seabeds (Storms et al., 2008; Lorenzo-Trueba and Ashton, 2014). During transgression along high gradient (>0.001) topography, the landward movement of the shoreline is relatively slow and erosion by wave action has more time to rework and redeposit sediments (Cattaneo and Steel, 2003). This results in shoreface retreat, the formation of a ravinement surface and relatively thick transgressive deposits above the ravinement surface (Cattaneo and Steel, 2003). The cited authors consider these conditions unfavorable for the drowning of a barrier complex, which in turn are likely to be preserved on a low-gradient shelf associated with a high rate of sea-level rise (Sanders and Kumar, 1975; Rampino and Sanders, 1980; Cattaneo and Steel, 2003). On the other hand, the high rate of sediment supply is considered a main driver in barrier overstep (Storms and Swift, 2003). This factor could be relevant for the overstepping of the deeper seaward barriers (Br1 and Br2), which were formed when the river mouth was probably located in the barrier island sector (Fig. 12C). With the sea level rise the wide backbarrier region was flooded forming a wide lagoon and the river mouth probably shifted landward the lagoon basin (Fig. 12D). At this stage the river sediments were presumably deposited in the inner lagoon shore and in the lagoon basin with a reduction of the sediment supply to the barrier islands.

Barrier preservation associated with a high seabed gradient (0.3°–0.4°) and a relatively low rate of sea-level (10–15 mm y^{-1}) can be linked to the early diagenetic processes which lead to rapid cementation and the formation of beachrocks, and subsequently to overstepping with the rise in sea level (Fig. 12 C–D). Without the occurrence of early cementation, the barrier deposits would probably be eroded by waves. Preservation of barriers related to early cementation was also found in several sites in eastern South Africa — the continental shelf offshore Durban (Green et al., 2013, 2014) and the KwaZulu-Natal shelf (Salzmann et al., 2013). In these case studies, the barrier formation was associated with a standstill in sea-level rise, cementation was found to occur over a short period as the barriers were forming, and overstepping was related to a rapid increase in the sea-level rate associated with meltwater pulses (Green et al., 2013; Salzmann et al., 2013).

Barriers of the present case study evolved under a constant rate of sea-level rise (10–15 mm y^{-1}). Observed barrier elevation and preservation increased landward. The deepest barrier (Br1) was almost completely destroyed and only a relict of the paleomorphology is visible. Barriers Br2 and Br3 are well preserved, and are respectively of 2.5 and 5.1 m height, considering the difference in elevation between the top and the seaward toe. It can be estimated that a sea-level elevation of 11 m (from 29 to 18 m of depth below present s.l.), over a period of 1 ka, allowed for the formation, cementation overstepping and complete drowning of barriers Br2 and Br3, which are composed of several alignments of single barriers. The sea-level elevation which allowed to the formation of single barriers (e.g. Br2a and Br2b) can be estimated in the order of 2–3 m over a period of 0.1–0.2 ka. The only features which were preserved in the barrier island sector were the cemented barriers, without evidence of lagoon deposits among the barriers due to the low accommodation space.

The present case study exhibits a specific evolutionary model compared to the other systems described in the literature. Contrary to the Hasting banks (Mellett et al., 2012) the phase of barrier breakdown is negligible here, and preservation of the barrier–lagoon system is due to early cementation and sediment accommodation due to the topography of the back-barrier region rather than by an increase in the rate of sea-level rise over a low gradient shelf (Rampino and Sanders, 1980; Cattaneo and Steel, 2003; Storms et al., 2008).

The comparison of the present case study with the scenarios of future coastal flooding suggests that the rate of sea-level rise (10–15 mm y^{-1}) which occurred during the drowning of the ancient barrier–lagoon system is comparable to the maximum rates estimated by Church et al. (2013) (10 mm y^{-1}) and by Rahmstorf (2007) (15 mm y^{-1}) for coastal flooding up to the year 2100. The sea level rise of 1.5 m expected for the future over a time period of 0.1 ka is comparable to the sea level rise which occurred during the evolution of the ancient barrier system. Particularly differences of sea-level in the order of 2–3 m over 0.1–0.2 ka can be associated with the overstepping of barriers Br2a and Br2b and barriers Br3a and Br3b.

In the case of the present day barrier system of the Mistras lagoon (Fig. 11), the wide back-barrier space, the low gradient, the low wave energy and the low sediment input would suggest a readjustment of the new shoreline through a barrier migration involving sediment-deficit overstepping (Mellett et al., 2012) rather than continuous retreat. In this case, the formation time for the new barrier could be evaluated in the order of magnitude of centuries based on the ancient analogue and previous studies (Orford et al., 2002).

6. Conclusions

A well-preserved barrier–lagoon system, comprising several barriers in a depth range of 18–37 m and a wide back-barrier basin, developed on the western Sardinia shelf at the entrance of the Gulf of Oristano during the early Holocene. Barriers were formed and retreated through overstepping, their formation, evolution and preservation were mainly dictated by the inherited topography and the early barrier cementation.

Despite the relatively high seabed gradient (0.3°–0.4°) and relatively low rate of sea-level rise (10–15 mm y^{-1}), the barriers were not fully reworked and their shapes seem to be well preserved. This was due to early diagenetic processes which led to rapid cementation with the formation of beachrocks, and to subsequent overstepping with the rise in sea level.

The accommodation space in the back-barrier region was related to a large depression due to the incision of the river and the subsequent valley formation, and was additionally dictated by tectonics. Following the rise in sea level and the barrier formation, this depression was filled by lagoon and deltaic sediments, washover fans and beach deposits. The whole system evolved over a time period of 1 ka. The time associated with the formation and drowning of single barriers was estimated to be in the order of centuries.

Acknowledgments

This study was funded by the RITMARE Flagship Project funded by the Italian Ministry of Education, Research and Universities. The authors acknowledge Paolo Scotto, Alessandro Conforti, Sara Innangi and Gabriella Di Martino for their technical support with the vibrocore collection and geophysical data acquisition. The English text was revised by Katie Duff.

References

Antonioli, F., Ferranti, L., Lo Schiavo, F., 1997. The submerged Neolithic burials of the grotta Verde at Capo Caccia (Sardinia, Italy): implications for the Holocene sea-level rise. Mem. Descr. Serv. Geol. Naz. 52, 329–336.

Antonioli, F., Anzidei, M., Lambeck, K., Auriemma, R., Gaddi, D., Furlani, S., Orrù, P., Solinas, E., Gaspari, A., Karinja, S., Kovav, Surace, L., 2007. Sea-level change in Italy during the Holocene, from archaeological and geomorphological data. Quat. Sci. Rev. 26, 2463–2486.

Belknap, D.F., Kraft, J.C., 1981. Preservation potential of transgressive coastal lithosomes on the US Atlantic shelf. Mar. Geol. 42, 429–442.

Carboni, S., Lecca, L., 1985. Osservazioni sul Pleistocene Medio-superiore della penisola del Sinis (Sardegna occidentale). Boll. Soc. Geol. Ital. 104, 459–477.
Carter, R.W.G., Forbes, D.L., Jennings, S.C., Orford, J.D., Shaw, J., Taylor, R.B., 1989. Barrier and lagoon coast evolution under differing relative sea-level regimes: examples from Ireland and Nova Scotia. In: Ward, L.G., Ashley, G.M. (Eds.), Physical Processes and Sedimentology of Siliciclastic-dominated Lagoonal Systems. Marine Geology 88, pp. 221–242.
Casula, G., Cherchi, A., Montadert, L., Murru, M., Sarria, E., 2001. The Cenozoic graben system of Sardinia (Italy): geodynamic evolution from new seismic and field data. Mar. Pet. Geol. 18, 863–888.
Cattaneo, A., Steel, R.J., 2003. Transgressive deposits: an overview of their variability. Earth Sci. Rev. 62, 187–228.
Catuneanu, O., 2006. Principles of Sequence Stratigraphy. Elsevier, Oxford (375 pp.).
Church, J.A., Clark, P.U., Cazenave, A., Gregory, J.M., Jevrejeva, S., Levermann, A., Merrifield, M.A., Milne, G.A., Nerem, R.S., Nunn, P.D., Payne, A.J., Pfeffer, W.T., Stammer, D., Unnikrishnan, A.S., 2013. Sea level change. Climate Change 2013: The Physical Science Basis. Contribution of Working Group I to the Fifth Assessment Report of the Intergovernmental Panel on Climate Change. Cambridge University Press, Cambridge, United Kingdom and New York, NY, USA.
Cucco, A., Perilli, A., De Falco, G., Ghezzo, M., Umgiesser, G., 2006. Water circulation and transport time scales in the Gulf of Oristano. Chem. Ecol. 22 (supplement 1), 307–331.
Davaud, E., Kindler, P., Martini, R., Strasser, A., 1991. Enregistrement des variations eustatiques dans des dépôts littoraux du Pleistocène supérieur (San Giovanni di Sinis, Sardaigne occidentale). Bull. Soc. Geol. Fr. 162, 523–533.
De Falco, G., Baroli, M., Murru, E., Piergallini, G., Cancemi, G., 2006. Sediment analysis evidences two different depositional phenomena influencing seagrass distribution in the Gulf of Oristano (Sardinia — western Mediterranean). J. Coast. Res. 22 (5), 1043–1050.
De Falco, G., Baroli, M., Cucco, A., Simeone, S., 2008. Intrabasinal conditions promoting the development of a biogenic carbonate sedimentary facies associated with the seagrass *Posidonia oceanica*. Cont. Shelf Res. 28 (6), 797–812.
De Falco, G., Tonielli, R., Di Martino, G., Innangi, S., Simeone, S., Parnum, I.M., 2010. Relationships between multibeam backscatter, sediment grain size, and *Posidonia oceanica* seagrass distribution. Cont. Shelf Res. 30, 1941–1950.
De Falco, G., Budillon, F., Conforti, A., Di Bitetto, M., Di Martino, G., Innangi, S., Simeone, S., Tonielli, R., 2015. Sorted bedforms over transgressive deposits along the continental shelf of western Sardinia (Mediterranean Sea). Mar. Geol. 359, 75–88.
Demuro, S., Orrù, P., 1998. Il contributo delle beach-rock nello studio della risalita del mare olocenico. Le beach-rock post-glaciali della Sardegna nord-orientale. Il Quaternario 11, 19–39.
Di Rita, F., Melis, R., 2013. The cultural landscape near the ancient city of Tharros (central West Sardinia): vegetation changes and human impact. Quat. Int. 40, 4271–4282.
Evans, M.W., Hine, A.C., Belknap, D.F., Davis Jr., R.A., 1985. Bedrock controls on barrier island development: west-central Florida coast. Mar. Geol. 63 (1–4), 263–283.
Ferranti, L., Antonioli, F., Amorosi, A., Dai Prà, G., Mastronuzzi, G., Mauz, B., Monaco, C., Orrù, P., Pappalardo, M., Radtke, U., Renda, P., Romano, P., Sansò, P., Verrubbi, V., 2006. Elevation of the last interglacial highstand in Italy: a benchmark of coastal tectonics. Quat. Int. 145–146, 30–54.
Forbes, D.L., Taylor, R.B., Orford, J.D., Carter, R.W.G., Shaw, J., 1991. Gravel–barrier migration and overstepping. Mar. Geol. 97 (3–4), 305–313.
Francolini, L., Lecca, L., Mazzei, R., 1990. La presenza del Pliocene inferiore nella piattaforma della Sardegna occidentale. Atti Soc. Tosc. Sci. Nat. Mem. Ser. A 97, 93–111.
Gardner, J.V., Dartnell, P., Mayer, L.A., Hughes-Clarke, J.E., Calder, B.R., Duffy, G., 2005. Shelf-edge deltas and drowned barrier–island complexes on the northwest Florida outer continental shelf. Geomorphology 64, 133–166.
Gardner, J.V., Calder, B.R., Hughes Clark, J.E., Mayer, L.A., Elston, G., Rzhanov, Y., 2007. Drowned shelf-edge deltas, barrier islands and related features along the outer continental shelf north of the head of De Soto Canyon, NE Gulf of Mexico. Geomorphology 89, 370–390.
Green, A.N., Cooper, J.A.G., Leuci, R., Thackeray, Z., 2013. An overstepped segmented lagoon complex on the South African continental shelf. Sedimentology 60, 1755–1768.
Green, A.N., Cooper, J.A.G., Salzmann, L., 2014. Geomorphic and stratigraphic signals of postglacial meltwater pulses on continental shelves. Geology 42, 151–154.
Hayes, M.O., 1979. Barrier island morphology as a function of tidal and wave regime. In: Leatherman, S.P. (Ed.), Barrier Islands. Academic Press, New York, pp. 1–27.
Hesp, P.A., Short, A.D., 1999. Barrier morphodynamics. In: Short, A.D. (Ed.), Handbook of Beach and Shoreface Morphodynamics. John Wiley & Sons, LTD, England, pp. 307–333.
Kindler, P., Davaud, E., Strasser, A., 1997. Tyrrhenian coastal deposits from Sardinia (Italy): a petrographic record of high sea levels and shifting climate belts during the last interglacial (isotopic substage 5e). Palaeogeogr. Palaeoclimatol. Palaeoecol. 133, 1–25.
Lambeck, K., Antonioli, F., Purcell, A., Silenzi, S., 2004. Sea-level changes along the Italian coast for the past 10,000 yrs. Quat. Sci. Rev. 23, 1567–1598.
Lambeck, K., Antonioli, F., Anzidei, M., Ferranti, L., Leoni, G., Scicchitano, G., Silenzi, S., 2011. Sea-level changes along the Italian coast during the Holocene and a projection for the future. Quat. Int. 232, 250–257.
Leatherman, S.P., Rampino, M.R., Sanders, J.E., 1983. Barrier island evolution in response to sea level rise; discussion and reply. J. Sediment. Res. 53 (3), 1026–1033.
Lecca, L., 2000. La piattaforma continentale miocenico–quaternaria del margine occidentale sardo: blocco diagramma sezionato. Rend. Semin. Fac. Sci. Univ. Cagliari 70 (1), 49–70.
Long, A.J., Waller, M.P., Plater, A.J., 2006. Coastal resilience and late Holocene tidal inlet history: the evolution of Dungeness Foreland and the Romney Marsh depositional complex (U.K.). Geomorphology 82 (3-4), 309–330.
Lorenzo-Trueba, J., Ashton, A.D., 2014. Rollover, drowning, and discontinuous retreat: distinct modes of barrier response to sea-level rise arising from a simple morphodynamic model. J. Geophys. Res. Earth Surf. 119, 779–801.
Mariani, P., Braitenberg, C., Antonioli, F., 2009. Sardinia coastal uplift and volcanism. Pure Appl. Geophys. 166, 1369–1402.
Mauz, B., Vacchi, M., Green, A., Hoffmann, G., Cooper, A., 2015. Beachrock: a tool for reconstructing relative sea level in the far-field. Mar. Geol. 362, 1–16.
Mellett, C.L., Hodgson, D.M., Mauz, B., Lang, A., Selby, I., Plater, A.J., 2012. Preservation of a drowned gravel barrier complex: a landscape evolution study from the northeastern English Channel. Mar. Geol. 315–318, 115–131.
Mitchum, J.R., Vail, P.R., Sangree, J.B., 1977. Stratigraphic interpretation of seismic reflection pattern in depositional sequences. In: Payton, C.E. (Ed.), Seismic Stratigraphy—Applications to Hydrocarbon Exploration. AAPG Memoirs 26, pp. 117–134.
Molinaroli, E., Guerzoni, S., De Falco, G., Sarretta, A., Cucco, A., Como, S., Simeone, S., Perilli, A., Magni, P., 2009. Relationships between hydrodynamic parameters and grain size in two contrasting transitional environments: the Lagoons of Venice and Cabras, Italy. Sediment. Geol. 219, 196–207.
Nummedal, D., Swift, D.J.P., 1987. Transgressive stratigraphy at sequence-bounding unconformities: some principles derived from Holocene and Cretaceous examples. In: Nummedal, D., Pilkery, O.H., Howard, J.D. (Eds.), Sea-level Fluctuation and Coastal Evolution. SEPM Special Publication vol. 41, pp. 241–260.
Orford, J.D., Forbes, D.L., Jennings, S.C., 2002. Organisational controls, typologies and time scales of paraglacial gravel-dominated coastal systems. Geomorphology 48, 51–85.
Orrù, P., Solinas, E., Puliga, G., Deiana, G., 2011. Palaeo-shorelines of the historic period, Sant'Antioco Island, south-western Sardinia (Italy). Quat. Int. 232, 71–81.
Orrù, P., Mastronuzzi, G., Deiana, G., Pignatelli, C., Solinas, E., Spanu, P.G., Zucca, R., 2014. Sea level changes and geoarchaeology between the bay of Capo Malfatano and Piscinnì Bay (SW Sardinia) in the last 4 kys. Quat. Int. 336, 180–189.
Otvos, E.G., 2012. Coastal barriers — nomenclature, processes, and classification issues. Geomorphology 139–140, 39–52.
Pilkey, O.H., Cooper, A.G., Lewis, D.A., 2009. Global distribution and geomorphology of fetch-limited barrier islands. J. Coast. Res. 25, 819–837.
Rahmstorf, S., 2007. A semi-empirical approach to projecting future sea-level rise. Science 315, 368–370.
Rampino, M.R., Sanders, J.E., 1980. Holocene transgression in south-central Long Island, New York. J. Sediment. Petrol. 50, 1063–1080.
Rampino, M.R., Sanders, J.E., 1982. Holocene transgression in south-central Long Island, New York—reply. J. Sediment. Petrol. 53, 1020–1025.
Rampino, M.R., Sanders, J.E., 1983. Barrier island evolution in response to sea level rise: reply. J. Sediment. Petrol. 53, 1031–1033.
Roy, P.S., Cowell, P.J., Ferland, M.A., Thom, B.G., 1994. Wave-dominated Coasts. Coastal Evolution: Late Quaternary Shoreline Dynamics. In: Carter, R.W.G., Woodroffe, C.D. (Eds.), Cambridge University Press, Cambridge, pp. 121–185.
Salzmann, L., Green, A., Cooper, J.A.G., 2013. Submerged barrier shoreline sequences on a high energy, steep and narrow shelf. Mar. Geol. 346, 366–374.
Sanders, J.E., Kumar, N., 1975. Evidence of shoreface retreat and in-place "drowning" during Holocene submergence of barriers, shelf off Fire Island, New York. Geol. Soc. Am. Bull. 86, 65–76.
Schumm, S.A., 1993. River response to base level change: implication for sequence stratigraphy. J. Geol. 101, 279–294.
Shan, X., YU, X., Clift, P.D., Tan, C., LI, S., Wang, Z., SU, D., 2015. Ground-penetrating radar study of beach-ridge deposits in Huangqihai Lake, North China: the imprint of washover processes. Front. Earth Sci. http://dx.doi.org/10.1007/s11707-015-0501-z (in press).
Simeone, S., De Falco, G., Quattrocchi, G., Cucco, A., 2014. Morphological changes of a Mediterranean beach over one year (San Giovanni Sinis, western Mediterranean). J. Coast. Res. (Special Issue No. 70), 217–222.
Storms, J.E.A., Swift, D.J.P., 2003. Shallow marine sequences as the building blocks of stratigraphy: insights from numerical modeling. Basin Res. 15, 287–303.
Storms, J.E.A., Weltje, G.J., Terra, G.J., Cattaneo, A., Trincardi, F., 2008. Coastal dynamics under conditions of rapid sea-level rise: Late Pleistocene to Early Holocene evolution of barrier–lagoon systems on the northern Adriatic shelf (Italy). Quat. Sci. Rev. 27 (11–12), 1107–1123.
Stuiver, M., Reimer, P.J., Reimer, R., 2014. Calib radiocarbon calibration, execute version 7.1 html. http://calib.qub.ac.uk/calib.
Stutz, M.I., Pilkey, O.H., 2011. Open-ocean barrier islands. Global influence of climatic, oceanographic, and depositional settings. J. Coast. Res. 27, 207–222.
Swift, D.J.P., 1968. Coastal erosion and transgressive stratigraphy. J. Geol. 76, 444–456.
Swift, D.J.P., 1975. Tidal sand ridges and shoal retreat massifs. Mar. Geol. 18, 105–134.
Swift, D.J.P., Moslow, T.F., 1982. Holocene transgression in south-central Long Island, New York—discussion. J. Sediment. Petrol. 53, 1014–1019.
Ulzega, A., Hearty, P.J., 1986. Geomorphology, stratigraphy and geochronology of Late Quaternary marine deposits in Sardinia. Z. Geomorphol. 62, 119–129.
Vousdoukas, M.I., Velegrakis, A.F., Plomaritis, T.A., 2007. Beachrock occurrence, characteristics, formation mechanisms and impacts. Earth Sci. Rev. 85, 23–46.
Zecchin, M., Gordini, E., Ramella, R., 2015. Recognition of a drowned delta in the northern Adriatic Sea, Italy: stratigraphic characteristics and its significance in the frame of the early Holocene sea-level rise. The Holocene 25 (6), 1027–1038.